ACS Catalysis

Research Article

pubs.acs.org/acscatalysis

Methyl Formate Formation from Methanol Oxidation Using Supported Gold−Palladium Nanoparticles

Gareth T. Whiting,[†] Simon A. Kondrat,[†] Ceri Hammond,[†] Nikolaos Dimitratos,[†] Qian He,[‡] David J. Morgan,[†] Nicholas F. Dummer,[†] Jonathan K. Bartley,[†] Christopher J. Kiely,[‡] Stuart H. Taylor,[†] and Graham J. Hutchings*[,†]

[†]Cardiff Catalysis Institute, School of Chemistry, Cardiff University, Main Building, Park Place, Cardiff, CF10 3AT, United Kingdom

[‡]Department of Materials Science and Engineering, Lehigh University, 5 East Packer Avenue, Bethlehem, Pennsylvania 18015, United States

Supporting Information

ABSTRACT: Recent advances in the oxidation of alcohols to methyl esters using metal nanoparticles have paved the way for more environmentally benign processes, operating at lower reaction temperatures with high product selectivity. Here, we demonstrate the use of bimetallic 1 wt % Au−Pd/TiO_2 catalysts that achieve high activity for the oxidation of methanol to methyl formate at low temperature. The application of a water extraction treatment to retain size-stabilized Au−Pd nanoparticles, in contrast to a more standard thermal treatment, provides the most active catalyst for this reaction. Using in situ DRIFTS, we demonstrate that in situ activation during methanol oxidation enhances the catalytic activity at low temperature and that this is a long-lived effect. Surface adsorbates, particularly formate species, build up on the catalyst surface during the reaction and are proven vital to enhancing the catalytic effect.

KEYWORDS: *methanol, methyl formate, oxidation, gold−palladium, nanoparticles, active species*

1. INTRODUCTION

Current interest in the production of methyl esters is in large part due to their important use as biofuels,[1−4] but also because of their valuable applications in the synthetic fabric and fragrance industries. At present, methyl formate is produced commercially by the carbonylation of methanol, catalyzed by sodium methoxide, at temperatures around 80 °C, achieving 95% selectivity with low methanol conversion (30%).[5] The major disadvantage of this process, however, is the deactivation of the catalyst caused by impurities in the reagents, leading to undesirable side-products. This has stimulated a desire for the development of an alternative process. The aerobic oxidation of methanol to methyl formate has been reported on supported Ru[6,7] and Pd[8−10] catalysts, both of which are active at reasonably low reaction temperatures (30−130 °C), showing promise for the efficient production of this desirable organic compound.

Because of the current climate involving the need for more environmentally benign processes, the use of Au- and Pd-based catalysts for the aerobic oxidation of alcohols has become prominent,[11−17] offering (i) high product selectivity, which limits the need for byproduct waste removal, and (ii) low reaction temperatures, providing energy efficiency, each of which contributes to the ideals of "green" chemical processes. Recently, it was revealed that a nanoporous Au monolithic catalyst is highly active in the selective gas-phase oxidative coupling of methanol at temperatures as low as 20 °C, using O_2 as an oxidant.[18] Theoretical studies on single crystal Au (111) surfaces have demonstrated that the cross-coupling of methanol and formaldehyde is promoted by oxygen bound to Au surface sites under ultrahigh vacuum conditions.[19] The proposed mechanism of this complex reaction by Friend et al. may provide an explanation for the remarkable activity of Au catalysts. The initial adsorption of methanol on Au sites leads to the formation of chemisorbed methoxy species due to the weak −OH bond and the prevalent Au−O bond formed, and this is followed by β−H elimination to form adsorbed formaldehyde. The weak binding of the formaldehyde with the Au surface facilitates the coupling reaction with a neighboring methoxy species, producing methyl formate. The use of supported gold nanoparticles has also been reported as an effective catalyst in the oxidative coupling of alcohols,[20−22] with the oxide support playing a major role in supplying oxygen to the Au active center. A negative factor that can be significant when using supported metal catalysts is the propensity for sintering of the nanoparticles under both preparation and reaction conditions. This leads to growth of the nanoparticles and therefore results in a lower catalytic activity. The preparation of metal nanoparticles with a well-defined particle size distribution can be achieved using stabilizing ligands, such as poly(vinyl alcohol) (PVA)[23,24] or poly(vinylpyrrolidone) (PVP)[25,26] during the synthesis of the colloid sols, before

Received: May 9, 2014
Revised: December 9, 2014
Published: December 11, 2014

DOI: 10.1021/cs501728r
ACS Catal. 2015, 5, 637−644

immobilizing them on a support. The immobilization of the preformed nanoparticles on the support surface ensures precise control in particle size, giving an advantage in their use in catalytic processes, where metal nanoparticle size is a dominant factor in determining catalytic activity.[27]

The method of removal of stabilizing agents from the catalyst surface is key to influencing the effective size of the metal nanoparticles, with oxidative and thermal treatments commonly employed, because of the large quantity of ligand molecules that needs to be removed. There is a major drawback in the use of such methods, however, because extensive changes in the size and shape of the nanoparticles can occur during ligand removal, which partially undermines the motive for using the ligand in the first place.[28] We recently described an alternative method of removing the stabilizing ligand using a solvent extraction treatment.[27] This can, in some cases, remove sufficient quantities of the ligand while retaining the original nanoparticle size and more importantly, retaining metal particle morphology. The treatment of Au/TiO_2 and $Au–Pd/TiO_2$ catalysts with hot water for short periods of time was highly effective in removing PVA from the surface of the catalysts, thereby exposing more active sites. In comparison with the thermal treatment method, water-treated catalysts exhibited significantly enhanced activity in the oxidation of CO, benzyl alcohol, and glycerol, clearly demonstrating the effectiveness of the solvent extraction treatment. Comotti et al.[29] also noted that in situ activation of the ligand-stabilized catalyst provides a unique method to enhance its activity.

In this paper, we study catalytic properties of bimetallic $Au–Pd/TiO_2$ catalysts. These catalysts were prepared and treated using both solvent extraction and thermal treatments, and the activity of these catalysts for the oxidation of methanol to methyl formate is studied, giving insight into the nature of in situ activation and the role of surface species during the reaction.

2. RESULTS AND DISCUSSION

2.1. Methanol Oxidation Using $Au–Pd/TiO_2$. A 1 wt % $Au–Pd/TiO_2$ catalyst was prepared using the sol-immobilization method utilizing PVA as the stabilizing ligand. The material was then treated with one of the following routes: (a) refluxed in water at 90 °C for 60 min or (b) calcined in flowing air for 3 h at 200, 300, or 400 °C. It is known that such ligand removal procedures can affect the final size distribution of the supported particles.[27] For instance, the 1 wt % $Au–Pd/TiO_2$ water refluxed (90 °C, 60 min) sample presents a mean particle size of 2.6 nm (essentially identical to that of the untreated sample), whereas the sample calcined at 400 °C exhibits a mean size of 7.1 nm. However, given the milder conditions of the water reflux treatment, a greater amount of PVA remains on the catalyst surface in comparison with that of the calcined sample, which inevitably blocks some of the potential active sites.[27]

The nontreated and treated 1 wt % $Au–Pd/TiO_2$ catalysts were employed in the gas phase oxidation of methanol to methyl formate in a fixed-bed reactor, to determine the effect of nanoparticle size and residual PVA remaining on catalytic activity.

Figure 1 presents the conversion of methanol and methyl formate selectivity as a function of increasing reaction temperature for each catalyst. Most noteworthy is the moderate activity of the treated catalysts at 30 °C (~2.5% conversion), whereas the nontreated catalyst is inactive. Although the difference between the two catalysts at 30 °C is subtle, in the

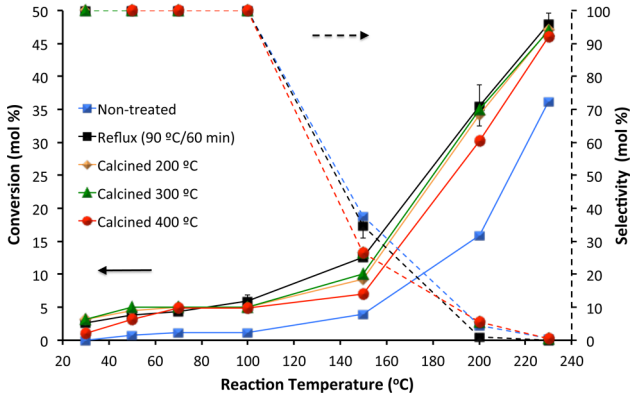

Figure 1. Effect of reaction temperature on methanol conversion (solid lines) and methyl formate selectivity (dashed lines) using $Au–Pd/TiO_2$ catalysts prepared using sol immobilization (reaction conditions: 5% MeOH; 2.5% O_2; 92.5% He, flow rate 60 mL min^{-1}).

context of the activity observed between 30 and 150 °C, the difference is significant. Upon increasing the reaction temperature to 150 °C, the apparent link of activity with nanoparticle size and the amount of PVA remaining on the surface becomes clearer. The water-refluxed catalyst obtains the highest conversion at this temperature (12.5%) in comparison with the other heat-treated and nontreated catalysts (calcd 300 °C, calcd 200 °C (10%); calcd 400 °C (7%); nontreated (3.5%)). Although the nontreated catalyst has the smallest mean nanoparticle size, its low reactivity (at reaction temperatures <200 °C) is to be expected, considering the greater amount of PVA remaining on the catalyst surface,[27] which blocks potential active sites. The opposite case is presented by the catalyst calcined at 400 °C, which has the least amount of PVA remaining on the surface but has by far the largest mean particle-size in the series of catalysts, and exhibits low activity at 150 °C. The selectivity toward methyl formate at 150 °C drops considerably, with an increase in CO_2 selectivity, suggesting the total combustion of methanol. This feature is enhanced further at higher reaction temperatures (i.e., >150 °C), with >90% selectivity to CO_2. Evidently, a correlation between nanoparticle size and amount of residual PVA remaining on the surface does exist, with smaller nanoparticle size and a lower PVA content being associated with higher activity. However, our 1 wt % $Au–Pd/TiO_2$ catalysts do not perform well at high reaction temperatures when methyl formate is the target product, and therefore, we should concentrate on the lower reaction temperatures for further discussion.

For the water-refluxed $Au–Pd/TiO_2$ catalyst, a 2.5% conversion and 100% methyl formate selectivity was achieved at 30 °C; however, this is not unexpected, with a recent article by Wang et al. also reporting the use of both monometallic Au and Pd and bimetallic Au–Pd nanoparticles supported on graphene for the selective oxidation of methanol to methyl formate at low temperature.[30] Using 3 wt % $Au_{(2.0)}–Pd_{(1.0)}$ nanoparticles, a methanol conversion of 90% and selectivity of 100% to methyl formate was achieved at a reaction temperature of 70 °C. Previously, Wittstock et al.[18] studied a leached nanoporous gold monolith as a catalyst for the partial oxidation of methanol, utilizing a methanol-to-oxygen molar ratio of 2:1, which is the same as that used in our study. They found higher activity at low temperatures: 10% conversion and 100% methyl formate selectivity at room temperature (~20 °C). This particular catalyst was formed by silver leaching from a gold–

DOI: 10.1021/cs501728r
ACS Catal. 2015, 5, 637–644

silver alloy, so this high activity may be due to the formation of a very dilute alloy of Ag in Au, with the Ag enhancing the activation of molecular oxygen. The activity we observe for the water refluxed Au−Pd/TiO_2 catalyst is therefore interesting and worthy of further investigation.

2.2. In Situ Activation of Au−Pd/TiO_2. Comotti et al.[29] have reported an interesting effect concerning the removal of the stabilizing ligand from catalysts prepared using sol immobilization. They observed that to achieve high activity, there is a requirement to thermally activate the catalyst under in situ reaction conditions. CO oxidation was studied using a 1 wt % Au/TiO_2 catalyst prepared using PVA as the stabilizing ligand. A 90% increase in activity was achieved after an in situ thermal activation. In view of this, we decided to explore this activation protocol in the present study. Given the large variations in particle size distribution and amount of PVA remaining on the metal surface, the following catalysts were selected to study their in situ activation for methanol oxidation: 1 wt % Au−Pd/TiO_2 (i) nontreated state, (ii) after water treatment (90 °C 60 min), and (iii) calcined at 400 °C.

The catalytic activity prior to and following in situ thermal activation for each sample set is shown in Figure 2a,b, respectively. The methyl formate selectivity observed at this conversion level is reported above each column. The retention of a similar activity level for the 400 °C calcined 1 wt % Au−Pd/TiO_2 catalyst before and after thermal activation is to be expected. This is because the major fraction of the PVA has already been removed during the calcination pretreatment prior to its use in the oxidation reactor; therefore, any further in situ heat treatment at 230 °C produces no effect, positive or negative, on the catalytic activity. In this case, catalytic activity is likely predetermined by the relatively broad particle size distribution. The nontreated 1 wt % Au−Pd/TiO_2 (dried at 120 °C) catalyst retains the highest PVA content on its surface compared with the calcined and refluxed catalysts, so its catalytic activity after in situ thermal treatment does not improve. This could be due to the substantial amount of PVA still blocking potential active sites (it is possible that a longer heat treatment time is required). The initial activity of the Au−Pd/TiO_2 water-refluxed catalyst at low reaction temperatures is moderate (Figure 2a); however, following in situ thermal activation, the catalytic activity below 100 °C is markedly enhanced (Figure 2b), achieving 25% methanol conversion and 60% methyl formate selectivity at 30 °C, with a TOF of 1.73 h^{-1}. The effect for the water-refluxed catalyst is shown in more detail in Supporting Information (SI) Figure S1, where it is apparent that the enhancement in low temperature activity can be retained even upon reheating for a further time period.

To determine if monometallic catalysts (water-refluxed) also experience a similar effect, the catalytic properties of a comparable series of monometallic 1 wt % Au- and Pd/TiO_2 catalysts were also studied. Figure 3 shows the catalytic reaction profile of monometallic Au- and Pd/TiO_2 catalysts, which do not show any comparable enhanced conversion at low reaction temperatures after in situ thermal activation. It is therefore evident that synergy plays an important role in the enhanced activity exhibited by Au−Pd/TiO_2 catalysts, as was similarly observed by Wang et al.[30] In this case, the substantially higher activity of the bimetallic catalysts over both the monometallic variants was attributed to the Au acting as an electron promoter for the electron-deficient Pd sites as a result of intimate alloy formation.

To ensure stability of the catalytic activity of the water refluxed Au−Pd/TiO_2 catalyst at 30 °C following the in situ thermal activation, the catalyst was held under these same reaction conditions for 20 h (Figure 4). Over this time period, there is only a slight decrease in methanol conversion from 25 to 20%, accompanied by a concurrent increase in methyl

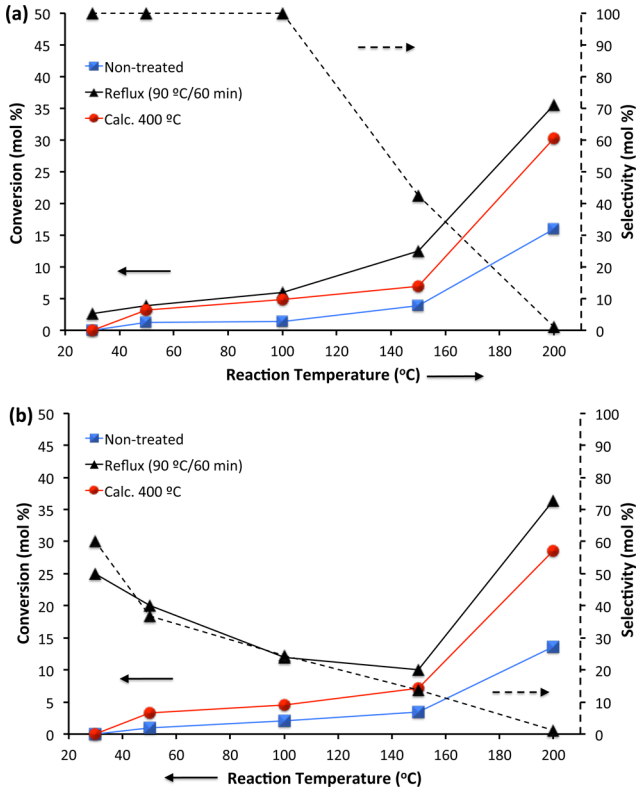

Figure 2. Activity prior to (a) and following (b) in situ activation during the oxidation of methanol to methyl formate using 1 wt % Au−Pd/TiO_2 catalysts prepared in the following way; nontreated, water-refluxed (90 °C 60 min), and calcined at 400 °C. A clear enhancement in catalytic activity at low reaction temperatures is observed for the water-refluxed catalyst after in situ activation (methyl formate selectivity noted at each reaction temperature for the water-refluxed treated catalyst only).

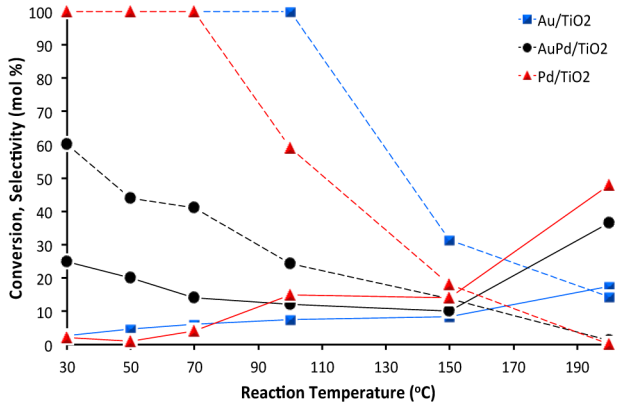

Figure 3. Oxidation of methanol to methyl formate following in situ thermal activation of monometallic 1 wt % Au- and Pd/TiO_2 catalysts and bimetallic 1 wt % Au−Pd/TiO_2 catalyst. Solid lines refer to methanol conversion, and dashed lines represent methyl formate selectivity.

DOI: 10.1021/cs501728r
ACS Catal. 2015, 5, 637−644

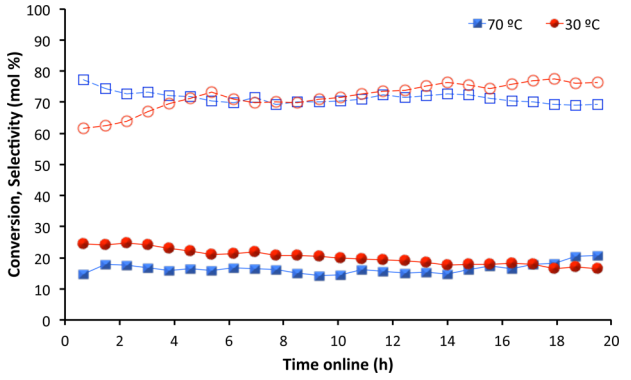

Figure 4. Stability investigation of in situ thermally activated 1 wt % Au−Pd/TiO_2 water-refluxed treated catalyst undergoing methanol oxidation at reaction temperatures of 30 and 70 °C for 20 h. Solid lines refer to methanol conversion and dashed lines represent methyl formate selectivity.

formate selectivity from 61 to 78%. This shows that this catalyst is stable over extended periods of time. However, at such low reaction temperatures, there is a possibility that methanol could be condensing on the surface of the catalyst, which could lead to a potential blocking of active sites over time. Therefore, the experiment was repeated and the reaction temperature was increased and held at 70 °C for 20 h following the initial in situ thermal activation (Figure 4). The activity of the catalyst remained stable over the entire reaction time period, achieving 15% methanol conversion and 70% methyl formate selectivity with a TOF of 1.17 h^{-1}.

2.3. Determining the Nature of the In Situ Activation Phenomena. *2.3.1. Nanoparticle Morphology and Surface Compositional Studies.* Interestingly, removing the 1 wt % Au−Pd/TiO_2 water-refluxed catalyst from the reactor (exposing to air) after the first heating treatment and cooling led to deactivation upon reuse (see SI Figure S2). Furthermore, an attempt to activate the catalyst by heating in static air to 230 °C outside of the reactor did not lead to the observed enhancement in low temperature activity. We therefore decided to first examine the structure and composition of various 1 wt % Au−Pd/TiO_2 materials refluxed in water at 90 °C related to this catalytic study; namely: (a) the fresh sample, (b) the catalyst after in situ activation up to 230 °C, and (c) the catalyst after ex situ treatment in static air up to 230 °C generated with the same temperature ramp sequence.

Examination by HAADF imaging in the scanning transmission electron microscope (Figure 5) does not show any significant differences in particle size distribution between these samples. The nanoparticle morphology is also found to be very similar to only a very small systematic increase in the mean particle size, but we do not consider that this is sufficiently significant to account for the large differences in catalytic activity observed between them. In addition, the fresh water-refluxed catalyst after use and the same sample after being subjected to a catalysis test cycle up to 230 °C (in situ activation) were also compared by STEM-XEDS analysis (Figure 6). All the metal nanoparticles are found to be homogeneous Au−Pd alloys exhibiting the same subtle systematic composition variations with particle size, with the smaller (2−3 nm) particles containing less Pd than the slightly larger (5 nm) nanoparticles. This same systematic trend in composition with particle size has been noted previously for supported Au−Pd alloys prepared by the sol-immobilization

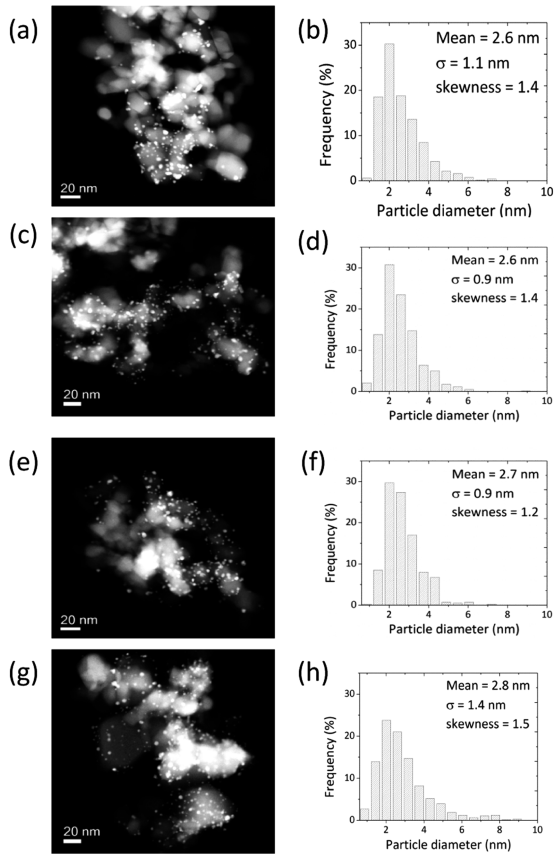

Figure 5. Representative HAADF images and the corresponding particle size distributions of 1 wt % Au−Pd/TiO_2 prepared by sol-immobilization with different post-treatments: (a, b) Fresh catalyst, (c, d) fresh catalyst after water-reflux treatment, (e, f) water-refluxed catalyst after in situ thermal activation, and (g, h) water-refluxed catalyst calcined ex situ at 230 °C (in situ activated).

method.[31] Hence, there was no discernible difference by STEM-XEDS analysis in the composition/particle size profiles of the freshly water refluxed sample and the same material after in situ activation to 230 °C.

The low reaction temperatures employed in the oxidation of methanol could, in principle, prevent desorption of products from the surface. In general, this effect would lead to a reduction in activity through product inhibition; however, in the present case, we observe that the sample that is activated in situ at 230 °C shows an increase in activity at low temperatures.

Investigation of the relevant surface species was conducted using XPS for the fresh and in situ activated 1 wt % Au−Pd/TiO_2 water refluxed catalysts. First, it should be noted that both gold and palladium have binding energies characteristic of their metallic states (see Table 1). The low binding energy of the gold is attributable to alloy formation and particle size effects, as noted from our previous work on TiO_2 supported Au−Pd catalysts.[32] The Pd/Au ratio determined by XPS for both samples is also quite similar (1.03 and 0.98) and is consistent with the minimal compositional differences observed by STEM-XEDS analysis (Figure 6).

Comparing the O (1s) XPS spectra for both these catalysts, however, did reveal a marked difference (Figure 7). The fresh water-refluxed catalyst revealed three distinct oxygen signals centered at 529.7, 532.0, and 533.2 eV which can be a assigned to Ti−O, −OH, and surface carbonate species, respectively. The latter carbonate species was verified by the existence of a C

DOI: 10.1021/cs501728r
ACS Catal. 2015, 5, 637−644

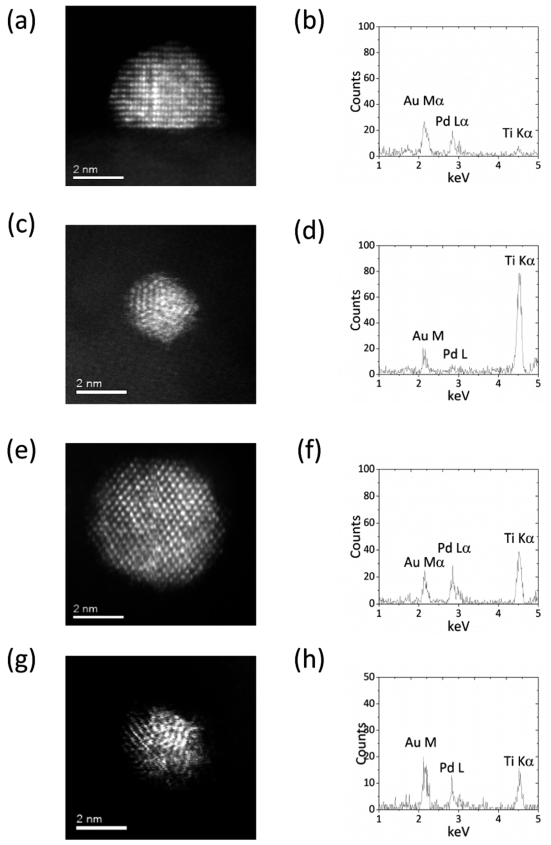

Figure 6. Representative HAADF image and corresponding XEDS point spectrum from (a, b) a 5 nm and (c, d) a 2 nm metal particle in a fresh 1 wt % Au−Pd/TiO_2 catalyst after reflux treatment. Representative HAADF image and corresponding XEDS point spectrum from (e, f) a 6 nm and (g, h) a 2 nm metal particle in a 1 wt % Au−Pd/TiO_2 catalyst after use in a catalysis test cycle up to 230 °C.

Table 1. XPS Analysis of the Surface Composition of a Fresh 1 wt.% Au−Pd/TiO_2 Catalyst, and a Postreaction 1 wt % Au−Pd/TiO_2 Catalyst Retrieved from the Methanol Oxidation Microreactor (in situ activated)

	XPS binding energy (eV)			
catalyst	Au 4f	Pd 3d	Ti 2p	O 1s
Au−Pd/TiO_2 (fresh)	83.1	334.8	458.5	529.7, 532.0, 533.2
Au−Pd/TiO_2 (used)	83.1	334.9	458.7	529.7, 531.5, 532.6, 533.4

(1s) peak at ∼289 eV. These signals are consistent with XPS analysis of fresh untreated TiO_2 as supplied by the manufacturer and are not a consequence of catalyst preparation. However, in situ activation has a notable effect on the O (1s) profile, and although signals pertaining to surface carbonate (533.2 eV) remain, the peak at 532 eV is replaced by two signals with energies of 531.5 and 532.6 eV. Given that it is entirely plausible that methoxy, formate, or other related species could be present on the catalyst surface, we can tentatively assign these binding energies to −OH/methoxy and O−C−O (formate-like) species, respectively.[33−37]

2.3.2. Mechanistic Insight from In Situ Spectroscopic Studies. To resolve the exact nature of the surface species responsible for increasing the activity of 1 wt % Au−Pd/TiO_2 catalyst after in situ activation, in situ DRIFTS studies were performed under near identical reaction conditions. At 30 °C,

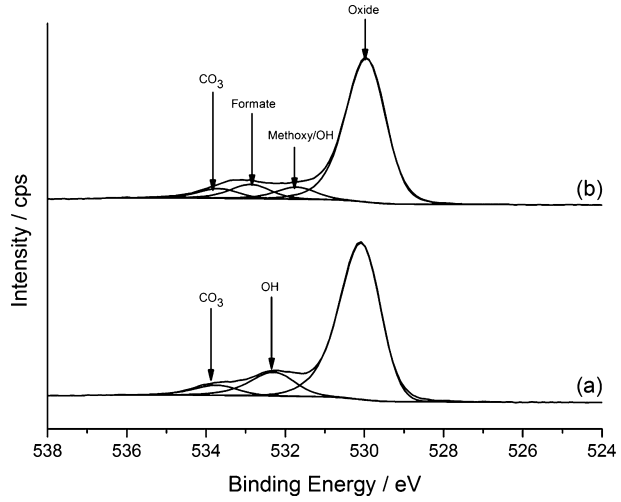

Figure 7. O(1s) core-level XPS spectra for (a) fresh and (b) in situ activated 1 wt % Au−Pd/TiO_2 catalysts.

multiple bands attributed to gaseous methanol dominate the spectra in the 3000−2800 and 1060−1040 cm^{-1} regions[38] (Figure 8a), with the negative band at 1650 cm^{-1} associated with the desorption of physisorbed water (OH) present on the fresh catalyst surface. Between the reaction temperatures of 50−100 °C, several bands form with increasing intensity. Those at 1150 and 1738 cm^{-1} are associated with methyl formate[38−40]

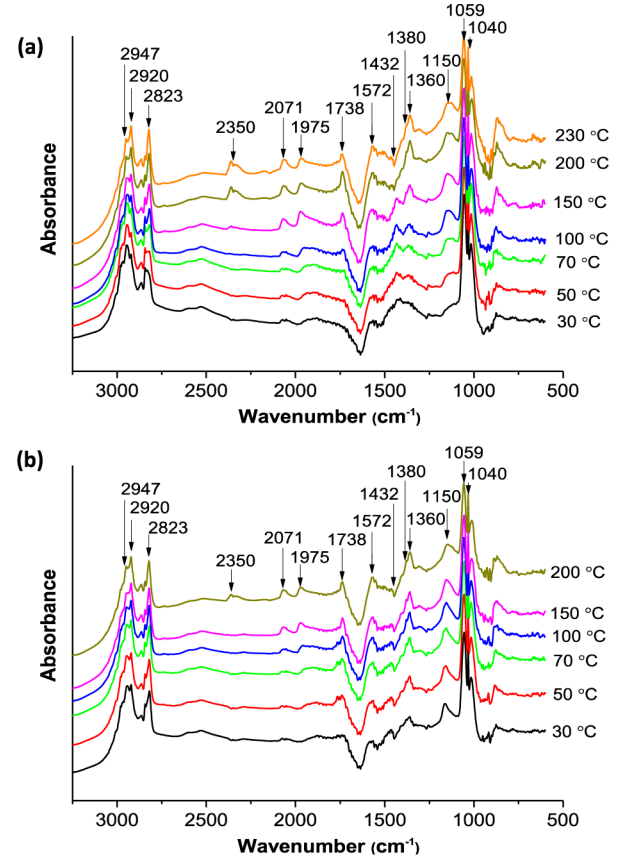

Figure 8. In situ DRIFT spectra of methanol oxidation over a 1 wt % Au−Pd/TiO_2 water-refluxed treated catalyst: (a) increasing reaction temperature (in situ activation) and (b) decreasing reaction temperature (following in situ activation).

DOI: 10.1021/cs501728r
ACS Catal. 2015, 5, 637−644

and become more prominent with increasing reaction temperature until 200 °C, where a decline in intensity is observed. This correlates similarly to catalytic testing (Figure 2), where a decrease in methyl formate selectivity is shown at temperatures of 150 °C and above. This was coupled with a concomitant rise in CO/CO_2 selectivity, which can also be seen in Figure 8a, with the appearance of bands at 2350 cm^{-1} (gaseous CO_2)[41] and 2017−1975 cm^{-1} (chemisorbed and physisorbed CO),[42] associated with the further oxidation of adsorbed intermediate compounds or methanol. Although gaseous methanol bands dominate the spectra in the 3000−2800 cm^{-1}region, additional bands visible at 2920 and 2823 cm^{-1}, assigned to methoxy species,[43,44] ($\nu_s(CH_3)$ and $2\delta_2(CH_3)$, respectively), form with increasing reaction temperature. As expected, this provides evidence that intermediate species exist on the catalyst surface during the reaction. Further intermediate species are also present in the form of adsorbed formate (ν_s(OCO) at 1380 and 1360 cm^{-1}, ν_{as}(OCO) at 1572 cm^{-1})[43−46] and formaldehyde ($\delta(CH_2)$ at 1432 cm^{-1} and $\gamma(CH_2)$ at 1059 cm^{-1}).[38] An additional notable feature of the band at 1432 cm^{-1} is its dramatic decrease in intensity at 200 °C, coupled with a significant rise of the band associated with formate ions (1360 cm^{-1}). This is due to the secondary oxidation of adsorbed formaldehyde molecules.[45]

Figure 8b displays the in situ DRIFT bands present/absent during the decrease in reaction temperature, mimicking the effect of in situ activation observed during catalytic testing (Figure 2). At 200 °C, a spectrum similar to that in Figure 8a is obtained; however, with a further decrease in reaction temperature, one should note a significant retention of several band intensities. Between 150 and 50 °C, bands attributed to methyl formate (1150, 1738 cm^{-1}), methoxy species (2920, 2823 cm^{-1}), and adsorbed formate (1572, 1360 cm^{-1}) maintain a high intensity in comparison with the corresponding spectra in Figure 8a. At 30 °C, each of the above bands remains, with only a slight decrease in intensity of each. SI Figure S3 compares the DRIFT spectra of the fresh and in situ activated catalyst at 30 °C (methanol bands subtracted), more clearly presenting the residual bands associated with surface species in the latter.

By referring to the mechanistic insight provided by in situ DRIFT spectroscopy, accompanied by catalytic testing data, we are now in a position to postulate the role of surface species on the observed in situ activation phenomena.

The mechanism of methanol oxidation to methyl formate over Au-based catalysts has been thoroughly investigated by Friend and co-workers in recent years.[47−50] It is now known that the first step is the O assisted O−H bond activation of methanol, forming adsorbed methoxy species. It is expected that in our supported catalysts, this oxygen species will be supplied at the support/nanoparticle perimeter or on defect sites.[51] Adsorbed methoxy species undergo β-H transfer with a neighboring O atom on the surface, forming adsorbed formaldehyde species. At this point, the surface contains the necessary reactant/intermediate species (if in close proximity) to form methyl formate. Understandably, these are lacking on the surface of the fresh catalyst, explaining the low reactivity at 30 °C. However, it should also be noted that residual PVA remaining on the surface of the fresh catalyst may also contribute to the low reactivity.

With an increase in the reaction temperature up to 100−150 °C, methanol is converted to a greater extent, as expected (Figure 2), and is accompanied by a rise in band intensity associated with adsorbed intermediate species—methoxy (2920, 2823 cm^{-1}), formate (1572, 1380, 1360 cm^{-1}), and formaldehyde (1432, 1059 cm^{-1})—along with the product, methyl formate (1738, 1150 cm^{-1}).

The presence of adsorbed formate molecules during the oxidation of methanol to methyl formate is not uncommon, and these have been suggested to be created upon the reaction of surface oxygen with adsorbed formaldehyde.[40,45] This was also observed to some extent in the in situ DRIFT spectra, with a decrease in intensity of the formaldehyde band ($\delta(CH_2)$ 1432 cm^{-1}) in the 150−200 °C temperature range correlating to an increase in the formate bands (1572, 1380, and 1630 cm^{-1}); however, Millar et al. propose that upon nucleophilic attack of surface oxygen on adsorbed methyl formate, adsorbed formate and methoxy species form.[45]

The final step in the proposed mechanism by Friend and co-workers is the formation of methyl formate from the reaction of adsorbed formaldehyde and adsorbed methoxy species, which is reported to take place when the two are in close proximity on the reaction surface.[47−50] However, it is also known that formate molecules on the catalyst surface can react with methanol[52] to form methyl formate as an alternative route, suggesting the importance of formate species during the reaction.

At high reaction temperatures, as expected, methanol (as well as other compounds) undergoes total combustion; hence, the dramatic drop in methyl formate selectivity and the corresponding increase in methanol conversion and CO_2 selectivity.

Figure 2 shows that upon decreasing the reaction temperature inside the microreactor to 30 °C, the 1 wt % Au−Pd/TiO_2 reflux treated catalyst exhibited a remarkable increase in reactivity in comparison with the fresh catalyst. This finding can now be related to the retention of intermediate species on the catalyst surface during the reaction, on the basis of our in situ DRIFTS spectroscopic studies (Figure 8b). The remaining bands associated with methoxy, formate, and formaldehyde species remaining on the surface at 30 °C after in situ activation (SI Figure S3) insinuates their active role in obtaining high reactivity and methyl formate selectivity during the second reaction cycle. By reference against previously proposed reaction mechanisms to generate methyl formate, the link between the presence of these residual surface intermediates, in situ activation, and catalytic activity becomes more evident.

Concerning the retention/loss of activity upon leaving or removing the catalyst in/from the reactor before second use, in situ DRIFT studies were carried out to provide further insight. Figure 9 displays the DRIFT spectra of the used 1 wt % Au−Pd/TiO_2 catalyst under a flowing N_2 atmosphere for 1, 5, and 16 h (with H_2O present), thus replicating the conditions of leaving the catalyst in the reactor under He flow overnight (again with H_2O present). The substantial decrease over time in intensity of the bands at 1738 and 1155 cm^{-1}, attributed to methyl formate is to be expected, considering the termination of reaction conditions. However, this is also accompanied by a rise in intensity of bands at 1360, 1380 (ν_s(OCO), and 1580 cm^{-1} (ν_{as}(OCO)) assigned to adsorbed (unidentate) formate ions. It is entirely plausible that methyl formate undergoes hydrolysis to form formic acid, which when adsorbed on the surface produces unidentate formate species. This was also observed by Millar et al., who noted that methyl formate adsorbed on Cu/SiO_2 slowly decomposes overtime, with a concurrent rise in intensity of adsorbed formate bands.[40] The

DOI: 10.1021/cs501728r
ACS Catal. 2015, 5, 637−644

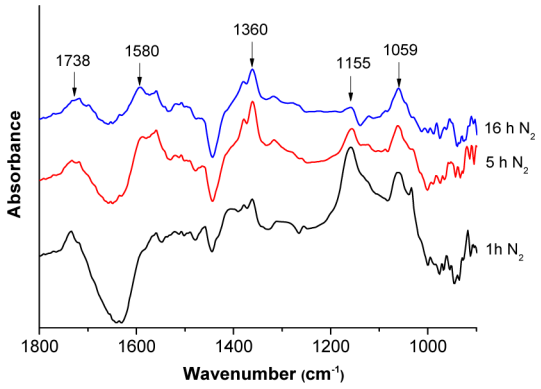

Figure 9. DRIFT spectra of a used (in situ activated) 1 wt % Au−Pd/TiO_2 (water-refluxed) catalyst treated under a N_2 flow (with H_2O present) as a function of time, to replicate leaving the catalyst in a reactor overnight under flowing He in the presence of H_2O.

retention/increased presence of formate ions on the surface that are available to react with methanol when normal reaction conditions are resumed explains the renewed high methanol conversion and methyl formate selectivity of the in situ activated catalyst.

This finding can also be used to explain the opposite trend in low activity of the in situ activated catalyst removed from the reactor (left in air overnight) prior to reuse. To replicate these conditions, the in situ activated catalyst was placed in static air for 16 h. This study revealed a noticeably lower intensity of bands associated with formate, with only weak bands at 1360 and 1059 cm^{-1} still being present (SI Figure S4). Therefore, an absence of these adsorbed surface intermediate species essentially relates to a "fresh" catalyst again, leading to low reactivity.

3. CONCLUSIONS

Supported bimetallic Au−Pd catalysts were demonstrated to achieve high activity at low reaction temperatures for the oxidation of methanol to methyl formate. The use of sol-immobilized 1 wt % Au−Pd/TiO_2 catalysts prepared using different water extraction and calcination treatments to remove PVA ligands was investigated, with several characterization techniques displaying a strong interplay between metal nanoparticle size, residual PVA ligand content, and catalytic activity. The bimetallic Au−Pd/TiO_2 catalyst washed with hot water demonstrated higher activity at low reaction temperatures than the corresponding calcined and nontreated catalysts. Remarkably, we observed that a subsequent in situ activation step leads to a significant enhancement in catalytic activity at low temperatures. Using in situ DRIFTS, we ascribed this effect to the increased quantity of adsorbates, particularly formate species, present on the catalyst surface.

■ ASSOCIATED CONTENT

Supporting Information

The following file is available free of charge on the ACS Publications website at DOI: 10.1021/cs501728r.

Materials and Methods, accompanied by figures supporting the main text (PDF)

■ AUTHOR INFORMATION

Corresponding Author

*E-mail: hutch@cf.ac.uk.

Notes

The authors declare no competing financial interest.

■ ACKNOWLEDGMENTS

We acknowledge the support of the Engineering and Physical Sciences Research Council (EP/E006345/1) of the U.K.

■ REFERENCES

(1) Adebowale, K. O.; Adewuyi, A.; Ajulo, K. D. *Int. J. Green Energy* **2012**, *9*, 297−307.
(2) Demirbas, A. *Prog. Energy Combust. Sci.* **2005**, *31*, 466−487.
(3) Tong, D.; Hu, C.; Jiang, K.; Li, Y. *J. Am. Oil Chem. Soc.* **2011**, *88*, 415−423.
(4) Moser, B. R. *Energy Fuels* **2008**, *22*, 4301−4306.
(5) Reutmann, W.; Keiczka, M. *Ullmann's Encyclopedia of Industrial Chemistry*, 5th Ed.; Wiley-VCH: New York, 1989; Vol. *A12*, p 13.
(6) Liu, H.; Iglesia, E. *J. Phys. Chem. B* **2005**, *109*, 2155−2163.
(7) Huang, H.; Li, W.; Liu, H. *Catal. Today* **2012**, *183*, 58−64.
(8) Lichtenberger, J.; Doohwan, L.; Iglesia, E. *Phys. Chem. Chem. Phys.* **2007**, *9*, 4902−4906.
(9) Cubeiro, M. L.; Fierro, J. L. G. *Appl. Catal., A* **1998**, *168*, 307−322.
(10) Wojcieszak, R.; Gaigneaux, E. M.; Ruiz, P. *ChemCatChem* **2012**, *4*, 72−75.
(11) Enache, D. I.; Edwards, J. K.; Landon, P.; S-Espriu, B.; Carley, A. F.; Herzing, A. A.; Watanabe, M.; Kiely, C. J.; Knight, D. W.; Hutchings, G. J. *Science* **2006**, *311*, 362−365.
(12) Tsunoyama, H.; Sakurai, Hi.; Negishi, Y.; Tsukuda, T. *J. Am. Chem. Soc.* **2005**, *127*, 9374−9375.
(13) Abad, A.; Almela, C.; Corma, A.; Garcia, H. *Tetrahedron* **2006**, *62*, 6666−6672.
(14) Buonerba, A.; Cuomo, C.; Sanchez, S. O.; Canton, P.; Grassi, A. *Chem.—Eur. J.* **2012**, *18*, 709−715.
(15) Abad, A.; Conception, P.; Corma, A.; Garcia, H. *Angew. Chem., Int. Ed.* **2005**, *44*, 4066−4069.
(16) Kosuda, K. M.; Wittstock, A.; Friend, C. M.; Bäumer, M. *Angew. Chem., Int. Ed.* **2012**, *51*, 1698−1701.
(17) Marx, S.; Baiker, A. *J. Phys. Chem. C* **2009**, *113*, 6191−6201.
(18) Wittstock, A.; Zielasek, V.; Biener, J.; Friend, C. M.; Bäumer, M. *Science* **2010**, *327*, 319−322.
(19) Liu, X. Y.; Madix, R. J.; Friend, C. M. *Chem. Soc. Rev.* **2008**, *37*, 2243−2261.
(20) Kegnæs, S.; Mielby, J.; Mentzel, U. V.; Christensen, C. H.; Riisager, A. *Green Chem.* **2010**, *12*, 1437−1441.
(21) Oliveira, R. L.; Kiyohara, R. K.; Rossi, L. M. *Green Chem.* **2009**, *11*, 1366−1370.
(22) Hvolbæk, B.; Janssens, T. V. W.; Clausen, B. S.; Falsig, H.; Christensen, C. H.; Nørskov, J. K. *Nano Today* **2007**, *2*, 14−18.
(23) Zhou, Y.; Wang, C. Y.; Zhu, Y. R.; Chen, Z. Y. *Chem. Mater.* **1999**, *11*, 2310−2312.
(24) Kesavan, L.; Tiruvalam, R.; Rahim, M. H. A.; Saiman, M. I. B.; Enache, D. I.; Jenkins, R. L.; Dimitratos, N.; Lopez-Sanchez, J. A.; Taylor, S. H.; Knight, D. W.; Kiely, C. J.; Hutchings, G. J. *Science* **2011**, *331*, 195−199.
(25) P-Santos, I.; L-Marzán, L. M. *Langmuir* **2002**, *18*, 2888−2894.
(26) Jaramillo, T. F.; Baeck, S.-H.; Cuenya, B. R.; McFarland, E. W. *J. Am. Chem. Soc.* **2003**, *125*, 7148−7149.
(27) Lopez-Sanchez, J. A.; Dimitratos, N.; Hammond, C.; Brett, G. L.; Kesavan, L.; White, S.; Miedziak, P.; Tiruvalam, R.; Jenkins, R. L.; Carley, A. F.; Knight, D.; Kiely, C. J.; Hutchings, G. J. *Nat. Chem.* **2011**, *3*, 551−556.
(28) Grunwaldt, J. D.; Kiener, C.; Wögerbauer, C.; Baiker, A. *J. Catal.* **1999**, *181*, 223−232.
(29) Comotti, M.; Li, W.-C.; Spliethoff, B.; Schuth, F. *J. Am. Chem. Soc.* **2006**, *128*, 917−924.
(30) Wang, R.; Wu, Z.; Chen, C.; Qin, Z.; Zhu, H.; Wang, G.; Wang, H.; Wu, C.; Dong, W.; Fan, W.; Wang, J. *Chem. Commun.* **2013**, *49*, 8250−8252.

DOI: 10.1021/cs501728r
ACS Catal. 2015, 5, 637−644

(31) Pritchard, J.; Kesavan, L.; Piccinini, M.; He, Q.; Tiruvalam, R.; Dimitratos, N.; Lopes-Sanchez, J. A.; Carley, A. F.; Edwards, J. K.; Kiely, C. J.; Hutchings, G. J. *Langmuir* **2010**, *26*, 16568−16577.
(32) Sankar, M.; He, Q.; Morad, M.; Pritchard, J.; Freakley, S. J.; Edwards, J. K.; Taylor, S. H.; Knight, D. J.; Kiely, C. J.; Hutchings, G. J. *ACS Nano* **2012**, *6*, 6600−6613.
(33) Carley, A. F.; Owens, A. W.; Rajumon, M. K.; Roberts, M. W.; Jackson, S. D. *Catal. Lett.* **1996**, *37*, 79−87.
(34) Schön, G. *Surf. Sci.* **1973**, *35*, 96−108.
(35) Au, C. T.; Hirsch, W.; Hirschwald, T. *Surf. Sci.* **1989**, *221*, 113−130.
(36) Günther, S.; Zhou, L.; Imbihl, R.; Hävecker, M.; Knop-Gericke, A.; Kleimenov, E.; Schlögl, R. *J. Chem. Phys.* **2006**, *125*, 114709−114719.
(37) Kreikemeyer Lorenzoa, D.; Bradleyb, M. K.; Unterbergera, W.; Duncanb, D. A.; Lerotholib, T. J.; Robinson, J.; Woodruff, D. P. *Surf. Sci.* **2011**, *605*, 193−205.
(38) Wojcieszak, R.; Karelovic, A.; Gaigneaux, E. M.; Ruiz, P. *Catal. Sci. Technol.* **2014**, *4*, 3298−3305.
(39) Lochar, V. *Appl. Catal., A* **2006**, *309*, 33−36.
(40) Millar, G. J.; Rochester, C. H.; Waugh, K. C. *J. Chem. Soc. Faraday Trans.* **1991**, *87*, 2785−2793.
(41) Wilcox, E. M.; Roberts, G. W.; Spivey, J. J. *Catal. Today* **2003**, *88*, 83−90.
(42) Hayden, B. E.; Kretzschmar, K.; Bradshaw, A. M. *Surf. Sci.* **1985**, *155*, 553−566.
(43) Burcham, L. J.; Badlani, M.; Wachs, I. E. *J. Catal.* **2001**, *203*, 104−121.
(44) Burcham; Wachs, I. E. *Catal. Today* **1999**, *49*, 467−484.
(45) Xu, B.; Madix, R. J.; Friend, C. M. *Acc. Chem. Res.* **2014**, *47*, 761−772.
(46) Busca, G.; Lamotte, J.; Lavalley, J.-C.; Lorenzelli, V. *J. Am. Chem. Soc.* **1987**, *109*, 5197−5202.
(47) Xu, B.; Madix, R. J.; Friend, C. M. *J. Am. Chem. Soc.* **2010**, *132*, 16571−16580.
(48) Xu, B.; Haubrich, J.; Freyschlag, C. G.; Madix, R. J.; Friend, C. M. *Chem. Sci.* **2010**, *1*, 310−314.
(49) Xu, B.; Liu, X.; Haubrich, J.; Friend, C. M. *Nat. Chem.* **2010**, *2*, 61−65.
(50) Xu, B.; Haubrich, J.; Baker, T. A.; Kaxiras, E.; Friend, C. M. *J. Phys. Chem. C* **2011**, *115*, 3703−3708.
(51) Iizuka, Y.; Tode, T.; Takao, T.; Yatsu, K.; Takeuchi, T.; Tsubota, S.; Haruta, M. *J. Catal.* **1999**, *187*, 50−58.
(52) Yu, K. M. K.; Yeung, C. M. Y.; Tsang, S. C. *J. Am. Chem. Soc.* **2007**, *129*, 6360−6361.

DOI: 10.1021/cs501728r
ACS Catal. 2015, 5, 637−644